Accelerated Energy Capacity Measurement of Lithium-Ion Cells to Support Future Circular Economy Strategies for Electric Vehicles

Jakobus Groenewald, Research Fellow, WMG, University of Warwick, Coventry, CV4 7AL, UK

j.groenewald@warwick.ac.uk

Thomas Grandjean, Research Fellow, WMG, University of Warwick, Coventry, CV4 7AL, UK

T.Grandjean@warwick.ac.uk

James Marco, Reader, WMG, University of Warwick, Coventry, CV4 7AL, UK

James.marco@warwick.ac.uk[1]

[1] Corresponding Author

Abstract

Within the academic and industrial communities there has been an increasing desire to better understand the sustainability of producing vehicles that contain embedded electrochemical energy storage. Underpinning a number of studies that evaluate different circular economy strategies for the electric vehicle (EV) or Hybrid electric vehicle (HEV) battery system are implicit assumptions about the retained capacity or State of Health (SOH) of the battery. International standards and best-practice guides exist that address the performance evaluation of both EV and HEV battery systems. However, a common theme is that the test duration can be excessive and last for a number of hours. The aim of this research is to assess whether energy capacity measurements of Li-ion cells can be accelerated; reducing the test duration to a value that may facilitate further EOL options. Experimental results are presented that highlight it is possible to significantly reduce the duration of the battery characterisation test by 70% - 90% while still retaining levels of measurement accuracy for retained energy capacity in the order of 1% for cell temperatures equal to 25^0C. Even at elevated temperatures of 40^0C, the peak measurement error was found to be only 3%. Based on these experimental results, a simple cost-function is formulated to highlight the flexibility of the proposed test framework. This approach would allow different organizations to prioritize the relative importance of test accuracy verses experimental test time when grading used Li-ion cells for different end-of-life (EOL) applications.

Keywords

Lithium Ion battery, Electric Vehicle, Energy Capacity Measurement, Energy Storage System, End-of-Life, Circular Economy

Acknowledgements

This research is supported by Innovate UK through the ABACUS Project (Project Number: 38846-283215) in collaboration with the WMG Centre High Value Manufacturing (HVM) Catapult, Jaguar Land Rover, Potenza Technology and G+P Batteries.

Abbreviations

ADC	Analogue-to-digital converter
BEV	Battery Electric Vehicles
BMS	Battery management software
CC	Constant current
CV	Constant voltage
DOE	Department of Energy
EERE	Energy Efficiency and Renewable Energy
EOL	End-of-Life
ESS	Energy storage system
EV	Electric Vehicle
HEV	Hybrid electric vehicle
HVM	High Value Manufacturing
ICE	Internal combustion engine

INL	Idaho National Laboratory
LCA	Life-Cycle Assessment
NEDC	New European Drive Cycle
PHEV	Plug-in Hybrid Electric Vehicles
SOC	State of charge
SOH	State of Health
USABC	US Advanced Battery Consortium

1 Introduction

There has been considerable research published into the different designs and technology options that underpin the energy storage system (ESS) employed within new electric vehicle (EV) or hybrid electric vehicle (HEV) concepts. This includes the use of different battery chemistries [1], the design of the energy management control software [2–4] and the mechanical integration of the battery system within the vehicle [5]. The primary motivation is often to overcome the systems engineering challenge and to design an ESS with an energy density and power density that will enable the design of new vehicles with a driving range and dynamic performance commensurate with consumer expectations. In addition to improving *on-vehicle* metrics of energy density, power density and component cost, there has been an increasing desire to better understand the sustainability of producing vehicles that contain embedded electrochemical energy storage. Much of this research has been guided by circular economy principles. The term circular economy has come to embody any framework that advocates an alternative to the traditional linear economic model (make, use, dispose); retaining key resources within the supply chain for longer, extracting the maximum value from them whilst in use before embarking on a process of regenerating products and materials at the end of their service life [6].

Underpinning a number of studies that critically evaluate different circular economy strategies for the vehicle's ESS are implicit assumptions about the State of Health (SOH) of the battery [7–9] . The metric SOH is often used to quantify the residual energy capacity of the cell at a time (t = n), relative to when the battery was new (t = 0):

$$SOH = \frac{Q_{t=n}}{Q_{t=0}} \quad (1)$$

End-of-Life (EOL) for the vehicle's ESS has been defined as the battery having a SOH of 80% [7,10–13]. However, a number of studies highlight the apparent arbitrary nature of this threshold value. It is often argued that even at 80% SOH, there is still inherent value embedded within the ESS [13–15].

Research by [2,16] argues that a measure of battery SOH should be calculated by the battery management software (BMS) and made available to all stakeholders within the supply chain via standard diagnostic interfaces and vehicle communication networks. To maximize the efficiency of the EOL strategy and to facilitate the repair, remanufacture or reuse of the battery system, SOH measurements should be made available for each battery module that comprises the battery pack (Section 2.2 discusses, in greater detail, the architecture of a typical vehicle battery system and the methods employed to aggregate cells into modules and finally into complete packs). However, from a review of commercially available EVs and HEVs, it is clear that this is not always the case, for example: the BMS within the Tesla vehicle does not provide information on battery SOH that can be viewed by a third-party, independent from the manufacturer. Assessing the battery installation for degradation, requires the battery pack to be removed from the vehicle, physically opened (that in turn damages the mechanical structure of the pack) and individual modules tested for retained capacity and impedance to quantify their SOH. This challenge is compounded, since it is likely that vehicle batteries will be presented to the supply-chain with unknown provenience and with varying levels of functionality [17]. A challenge therefore exists for those stakeholders wishing to sort or grade used vehicle battery systems to ascertain the most appropriate circular economy strategy for the battery that may comprise of: battery repair, reuse, remanufacturing or materials recycling in order to maximise the capture of the battery's inherent value.

International standards and best-practice guides exist that address the performance evaluation requirements for the both EV and HEV battery systems. Each standard addresses different domain requirements for performance, robustness and safety and how testing should be undertaken at either a cell (i.e. IEC-62660 and ISO-12405) or system level (i.e. United States Council for Automotive Research (USABC) Electric Vehicle Battery Test Procedures Manual). Within the context of this research and in line with the need to better understand residual energy capacity to assess battery SOH, particular consideration is given to the recommended procedures for cell-level capacity measurement. Irrespective of the test standard followed, a common theme throughout is that the test duration, taking into account the time required for the cell to equilibrate after a change in ambient temperature or state of charge (SOC) can be excessive and last for a number of hours. For this reason, the authors argue that these test strategies are potentially prohibitive for a number of vehicle manufacturers and specialist energy storage suppliers wishing to sort or grade used vehicle battery systems to ascertain the most appropriate circular economy strategy for the battery.

The aim of this research is to assess whether energy capacity measurements of Li-ion cells can be accelerated, reducing the test duration to a value that may facilitate further EOL options for used EV and HEV battery systems. In addition, the research aims to quantify the trade-off between test accuracy and test time, potentially allowing stakeholders to optimise the evaluation strategy they employ within the context of their respective commercial sectors.

This paper is structured as follows; Section 2 provides an overview of the automotive market and ESS technology solutions currently employed. Section 3 discusses, in greater detail, different EOL strategies for automotive battery systems. Section 4 introduces the different international standards and best-practice guides that are often employed as the basis for battery

characterization. Section 5 discusses the experimental method derived to compress the time required to assess the retained energy capacity within the cell. Results, Discussions and Conclusions from this research are presented in Sections 6, 7 and 8 respectively.

2 Market and Technology Overview

2.1 Market Overview for Electrified Vehicles

A recent 2015 report by KPMG [18] highlights the potential for electrified vehicles to be between 11-15% of new vehicle sales within the EU and China by 2025. Within the US, the market may comprise 16-20% of vehicles over the next 10 years. These predictions are comparable to those cited in [15]. The article collates a number of studies and concludes that, by 2025, there will be in excess of 11 million EV sales worldwide, with approximately 6 million in North America (20% of new vehicle sales). While a number of sources predict rapid sales growth, there are variations in the predicted technology-mix that will underpin this. In particular, the relative sales of HEVs that typically employ a smaller battery system (e.g. Toyota Prius Plug-in Hybrid Electric Vehicles (PHEV), with a 4.4 kWh battery), compared to an EV (e.g. the Nissan Leaf or the BMW i3), which require larger batteries in the order of 24 kWh and 22 kWh respectively. Research presented in [12] predicts that in 2035 the number of available EOL batteries will range from 1.4 million in their pessimistic forecast to 6.8 million in the optimistic forecast with a middle forecast of 3.8 million. Their analysis concludes that this volume is sufficient to justify the capital investment required to enable remanufacturing, repurposing and recycling. Further, their study highlights that the number of available EOL batteries will be between 55% and 60% of the number of batteries needed for new EV and PHEV production.

2.2 Vehicle Energy Storage Systems

A consensus does not exist as to the optimal design of battery cell, in terms of both chemistry and form-factor, for use within automotive applications. There is significant research characterizing the different chemistries, including: Lithium Cobalt Oxide ($LiCoO_2$), Lithium Iron Phosphate ($LiFeP0_4$), Lithium Nickel Cobalt Manganese (NCM - $LiNi_xCo_yMn_xO_Z$) and Lithium Titanate Oxide (LTO - $LI_4Ti_5O_{12}$). The integration challenge associated with designing a complete ESS using either pouch cells or cylindrical 18650 cells is reported within [2,3,19]. In [2] and [19] the authors highlight how cell-to-cell variations and non-uniformity within the cell further complicates ESS integration. Whereas within [3] the authors discuss the instrumentation and on-line monitoring requirements that underpin the battery control software.

It is beyond the scope of this paper to discuss, in detail, the engineering challenges associated with the ESS; further information can be found within [3,20]. To illustrate the complexity within a real-world system, Table 1 presents an overview of the contents of the battery pack within the commercially available Nissan Leaf EV. The Nissan Leaf has a reported range of 109 miles over the New European Drive Cycle (NEDC). The complete battery assembly weighs 293 kg and contains 48 battery modules, each containing 4 Li-ion pouch cells. An active cooling system is not included within the battery, but it does contain an electrical heating element to warm the Li-ion cells. The 48 modules within the battery are grouped together into 3 primary sub-assembles called module stacks, each containing a number of electrical interfaces and mechanical fasteners. The module stacks are accessible once the pack lid has been removed, potentially making it easier to identify and replace faulty components during a repair or remanufacturing activity. The battery pack is held together and attached to the vehicle chassis using 20 mechanical bolts. Within the battery, at the module stack and module levels, a variety of different joining methods are employed, including mechanical screws and bolts, totaling 376 fasteners. It is noteworthy that adhesives or mechanical welds are not employed within the assembly which, as discussed within [10,21,22],

can significantly inhibit a number of EOL options for the ESS. The challenges associated with module disassembly due to battery tab welding are explored within [10], whereas the authors within [22] extend the discussion and highlight the importance of considering methods of cell-to-cell fastening and joining at the battery system design stage of the development process.

3 The Need for End of Life Strategies for Vehicle Battery Systems

A common view reported within the literature is that the sustainability of integrating resource intensive battery packs into vehicles is not clear. Embedding circular economy principles of reuse, remanufacturing and recycling is seen as one method to minimize production cost and environmental impact. Two of the primary concerns regarding the sustainability of electrified vehicles are the financial cost of the ESS and the associated environmental impact of the device during production, usage and recycling. The financial cost of the battery system is often cited as the primary barrier to EV production [14,15]. Within [14], the authors survey a number of business models for battery cost reduction, underpinned by greater sales volumes, towards 2020-2025. Conversely [15] highlights the importance of embedding circular activities for the battery as one means of amortizing battery costs over more than the first vehicle life. Research by [12] states that a 50% reduction in battery cost is required to equalize the economics of owning a PHEV as compared to a conventionally-fueled vehicle. Conversely, [15] show that the EV powertrain cost must reduce from circa: \$600-700 kWh^{-1} to \$200 kWh^{-1} to achieve parity with comparable internal combustion engine (ICE) technology. Different mitigation strategies for lowering life-cycle cost through recycling and remanufacturing have been discussed. The financial incentives associated with recycling different lithium-ion (Li-ion) battery chemistries is, however, not clear and is highly dependent on the chemistry employed [12,15]. The Life-Cycle Assessment (LCA) of electrified vehicles has been widely reported [14,15,23–25]. In [14] the authors highlight the positive impact that the re-use of 2nd life vehicle battery systems may have on a future grid storage market.

Research presented within [15] and [23] argues that life-extension for the battery is essential if the higher emissions, associated with initial battery manufacture, are to be mitigated. This is further explored within [23] that discusses the potential impact on the environment of battery recycling and the capabilities that existing within different geographical territories. A case-study that aims to draw together the different options for LCA for a typical PHEV is derived and presented within [25] and is subsequently employed as the basis for a number of different scenarios exploring the potential advantages of battery reuse, recycling and remanufacture. Common scenarios include the use of vehicle-to-grid (V2G) or the use of the vehicle's battery in 2nd-life applications in which different EOL batteries are aggregated together to form larger grid-storage solutions for meeting peak-power demand. One of the primary outputs from the LCA is a better understanding of the CO_2 emissions associated with ESS production as compared to in-vehicle use. For example, a conceptual 10kWh battery is discussed in [25] for use within a PHEV over 3000 charge-discharge cycles or 200,000 km of driving. For this scenario, approximately 45% of the equivalent carbon emissions ($CO2_{eq}$) are related to battery production with the balance coming from vehicle use. The ratio of CO_{2eq} between the production and usage phases can vary from between 30% - 70% if the vehicle is employed within different geographical regions that employ different technologies for electricity generation (e.g. China vs. Scandinavia). This is supported by a similar study [10] that reports the emitted CO_{2eq} for the production of an EV battery system is approximately twice that of an ICE vehicle and represents 35% of the combined emissions for both production and vehicle use.

The extraction of raw materials through recycling and the use of the battery in 2nd - life applications is widely documented. In contrast, there has been relatively little research published that investigates the requirements for remanufacturing the vehicle's battery system as an alternative EOL strategy. A number of possible definitions for remanufacturing exist within the

literature [26–28]. A common view is that a remanufactured product should be of the same quality as the remanufactured article [29]. In recent years, independent commercial organizations have arisen that claim to offer a battery remanufacturing service for the Nissan Leaf and the Toyota Prius. However, in all cases, the organizations only offer a limited warranty (circa: 12 months) and do not claim the vehicle will have a comparable performance to a newly purchased vehicle. It follows therefore that the services offered by independent commercial organizations are unlikely to be able to provide the *as new* capabilities required by the definition of remanufacturing. The potential volume of EVs that exists within the market is a key measure when considering different EOL strategies. This is discussed with [10,12], within the context of the installed energy capacity for new V2G applications and 2nd-life grid storage solutions. Within the context of remanufacturing, the potential volume of electrified vehicles underpins the *security of supply for the core.* As discussed further in [1,22,30], the concept of the remanufacturing core relates to the fundamental component or subsystem that undergoes the remanufacturing process. As discussed previously, a clear understanding of battery SOH underpins all EOL strategies. For example, within [7] a decision making model is formulated for different scenarios based on battery SOH. The model defines the optimum EOL strategy as remanufacturing for a cell with retained capacity between 100-80%; followed by reuse within a grid storage application for a SOH between 80-45%. Below this threshold the economics of the production process precludes further ESS repurposing and greatest economic benefit is recovered from material recycling.

4 Energy Capacity Measurement

4.1 Review of Academic Literature

A number of publications discuss the need to quantify the energy capacity within a battery cell [31–34] as a fundamental stage of assessing the appropriate EOL strategy for the battery, as discussed within the previous section, or for defining the battery SOC or SOH as part of the on-line

management of the battery system within an automotive [35] or grid storage application [36]. the challenge of measuring capacity retention is discussed within the context of cells subject to cyclic electrical loading [32] and those that experience capacity fade due to extended periods of storage [31]. Within [37] the authors highlight the different terms often employed for describing battery capacity, they include: *nominal capacity*, *initial capacity* or *actual capacity*. Nominal capacity is typically that cited by the manufacturer and relates to the discharge energy capacity of the cell under strict environmental conditions (e.g. 1C current, at a temperature of 25^0C). Initial capacity is defined as the energy capacity of the cell, when the cell is new and discharged from a fully charged state, to the defined cut-off voltage [37]. Actual capacity defines the energy that may be extracted from the cell (from a fully charged state) when the battery is aged or when the battery is being discharged under conditions that are different from those defined as nominal by the manufacturer. The influence of C-rate at a cell level and pack level and the impact of temperature on cell capacity measurement is widely reported [33,38,39]. Within [40], the authors describe an increase in measured capacity for cell temperatures in excess of 40^0C compared to when the battery is operated at lower temperatures. Similarly, within [41], the authors highlight the dependency between energy capacity and C-rate. At high C-rates, the lower voltage limit on the cell is reached sooner due to a combination of diffusion limitations within the electrode [42] and an increase ohmic related voltage drop [35]. A number of publications have cited the need to take into account hysteresis when quantifying cell capacity under combined charge-discharge conditions [40]. Within [36, 37] the authors discuss the need to take into account the voltage dynamics of the cell when quantify the open circuit voltage (OCV) as part of the capacity measurement procedure. Publications highlight the need to charge and discharge the battery at low C-rates (circa: C/3 or C/10) if an accurate representation of the OCV-SOC relationship is to be obtained. The need to quantify energy capacity is not constrained to a cell-level assessment. Within [45], the authors discuss the challenge of quantifying energy capacity for a complete

module assembly or battery pack, taking into account cell-to-cell variations [46] and the unmeasurable current flows that may occur within the battery module when cells are connected electrically in parallel [47]. A comprehensive review of different capacity (and thus SOC) estimation methods for inclusion within the BMS is presented within [3,48]. This survey of methods will not be repeated here. In part, because a number of these studies are focussed on quantifying the partial charge state of the battery, as opposed to defining the full capacity of the cell and are therefore not in scope. However, for completeness a short summary is provided. Methods for battery SOC estimation are broadly categorised into three groups. The first relates to simple column-counting [49] in which the charge throughput of the cell is numerically integrated with respect to time. Because of the errors associated with integrating current over an extended period, studies advocate combining column counting with voltage correction. Voltage correction methods, typically use the OCV-SOC characteristic, either measured off-line or estimated using a real-time model of the battery to more accurately define the partial charge state of the battery relative to the nominal or actual capacity. As discussed within [50,51] methods of estimation often employ different variants of the Kalman Filter technique. Finally, a data-driven approach may also be employed that uses behavioural or ageing models of the battery to estimate the capacity of the cell after a period of storage (e.g. calendar ageing) or electrical loading. Research, cited in [52], provides examples of complimentary studies that use artificial neural networks, fuzzy logic or statistical methods for estimating the value of cell energy capacity.

4.2 International Standards

Table 2 provides a detailed overview of both legislative and best-practice standards that address the performance evaluation requirements for both EV and HEV battery systems. Figure 1 presents the test duration (in hours) that is required to complete cell level energy capacity measurements from five key international standards. As it can be seen, the time requirements vary considerably

from circa: 11 hours for the International Standards Organization (ISO) 12405-1 Hi-Power applications standard, to 75 hours for the North American USABC standard. The primary reason for this divergence, is that the latter has repeated discharge rates at three different low C-rates during a charge optimization stage. Within all the standards, the test time includes that defined for thermal and electrochemical equilibrium to occur at each stage of the test process (e.g. during pre-conditioning, testing and post-conditioning). While the use of *wait times* is widely employed when a change of cell temperature or SOC is required, the standards presented in Table 2 rarely provide any rationale or justification for the values employed. For example, within the USABC tests, a wait-time is 1 hour is defined, conversely within QC/T 743-2006 (the characterization standard defined by the Chinese authority's for EV batteries sold in China) a time of 2 hours is defined after a change in cell SOC.

The authors acknowledge that within the context of laboratory or academic research, the need for such refinement and accuracy within the test methodology is fully justified. However, the authors argue that these test durations would be prohibitive for a number of vehicle manufacturers and specialist energy storage suppliers wishing to sort or grade used vehicle battery systems to ascertain the most appropriate circular economy strategy for the battery. This challenge is compounded when considering the potential volumes of vehicle batteries that may be on the market (discussed in Section 2.1), and the need to test vehicle batteries potentially at different levels of completeness (e.g. pack, module or cell level) and functionality. There are two primary means to accelerate the measurement of stored energy within a Li-ion cell, these are (a) to cycle the cell at higher C-rates and (b) to reduce the time allowed for the cell voltage to stabilise after each change in SOC. Section 5 discusses, in greater detail, the experimental test programme derived to quantify the trade-off between the accuracy of the energy capacity measurement and the ability to reduce the duration of the test.

5 Experimental Method

5.1 Cell Selection

Two cell types were selected for evaluation as part of this research; a commercially available pouch cell, designated as a *power cell* by the manufacturer for use within HEV applications and an 18650 *energy cell* for use within a BEV. Table 2 presents the pertinent electrical performance data for each cell. The chemistry of the 18650 cell was Lithium nickel cobalt aluminum oxide ($LiNiCoAlO_2$ or NCA) with a LiC_6 (graphite) anode. Conversely, the pouch cell was Lithium Nickel Manganese Cobalt Oxide ($LiNiMnCoO_2$ or NMC). These cells were selected because both cell formats are under investigation by a number of automotive OEMs researching the integration of energy storage within future EVs and HEVs. For example, commercially available EVs: Nissan Leaf and BMW i3 employ pouch cells, whereas Tesla favor the cylindrical 18650 option. Similarly, the battery chemistries under investigation are also being commercialized by vehicle OEMs and system integrators. For example, NCA is employed by Tesla and NMC by Nissan within the Leaf. The use of commercially available cell formats and chemistries underpins the relevance of the research undertaken and its potential impact within the broader industrial sector.

5.2 Experimental Facilities and Test Set-up

Figures 2(a) and 2(b) present a schematic representation of the experimental set-up and a photograph of the actual laboratory equipment employed. As it can be seen, it comprises of a host personal computer (PC), a Bitrode cell cycler and an Espec thermal chamber. From the manufacturer's literature, the resolution of the output current from the battery cycler is 5 mA. The terminal voltage of the cells was measured at a sample rate of 100 ms and at an accuracy of 50 mV/bit using the on-board 10-bit analogue-to-digital converter (ADC). The ambient temperature for the cells was controlled to the target temperature (defined in section 5.3) to an accuracy of +/-

1°C. Figure 2 (c) presents the mounting fixture employed to electrically connect the twelve cells under test to the Bitrode cycler. Given the electrical rating of the cell cycler (100 A at 5 V per channel), in order to meet the desired electrical loading (defined in section 5.3) each cell was driven from two output channels connected in parallel providing an effective capacity of 200 A at 5 V. Figure 3 defines the locations on the surface of both the pouch and the 18650 cells where thermal measurements were made during the accelerated capacity tests. T-type thermocouples were connected to the surface of the cells in the locations shown. Cell temperature was recorded at a sample rate of 1 Hz with an accuracy of 0.5% of the measured value.

5.3 Experimental Procedure

Figure 4 presents an overview of the experimental procedure followed. In order to assess the feasibility of reducing the test time associated with energy capacity measurements, three test vectors were employed for: cell temperature, the charge and discharge rate employed to cycle the battery and finally three different values of relaxation time allowed between successive charge and discharge events:

- Cell temperature = [0^0C, 25^0C, 40^0C];
- C-rate = [1C, $\frac{max-C}{2}$, max- C]
- Wait time = [60 minutes, 30 minutes, 0].

These measures were selected for investigation because they represent key parameters within many International Standards (e.g. ISO 12405:2014 and IEC EN62660:2010) that dictate the time duration of the test. The three test vectors allow for the definition of a Reference Measurement to be made (see Section 5.3.1) and then a series of sensitivity studies to be undertaken in which each of the three terms (cell temperature, C-rate and wait time) are perturbed from the nominal value. The range of values selected encapsulates the expected operating envelope of the battery technology within an automotive usage context. In total, 27 separate energy capacity

measurements on each of the 12 cells were made. Figure 5 presents the experimental test matrices employed and a subset of the test profile programmed within the battery cycler.

5.3.1 Reference Energy Capacity Measurement

Before the accelerated capacity measurements commence a reference capacity measurement for each cell was made using the recognized method defined in [44]. The temperature of each cell was set to 25^0 C and allowed to stabilize for 720 minutes. The cells were fully charged using a constant current (CC) of C/3 to the upper voltage defined by manufacturer followed by a constant voltage (CV) phase until the current reduced to C/65. The cells were allowed to rest for 180 minutes prior to being fully discharged at 1C to their respective lower voltage threshold. The energy extracted from the cells during the discharge was recorded as a measure of their 1C capacity.

5.3.2 Accelerated Energy Capacity Measurements

Using the thermal chamber, the temperature of each cell was set to the target value. Each cell was then electrically cycled from its minimum to the upper voltage value (e.g. 100% SOC) three times. For each charge-discharge cycle the rest time allowed for the cell voltage to equilibrate was successively reduced from 60 minutes, 30 minutes and then finally zero. After electrically loading the cell for a given C-rate (derived using the maximum C-rate of the cell defined in Table 3), the reference test (defined in Section 5.3.1) was completed again for each cell. By continually performing the reference test throughout the text matrix, it becomes possible to check for and to quantify any cell degradation (e.g. capacity fade) that may occur due to the higher current rates and reduced relaxation times. The presence of significant capacity fade would invalidate any comparison of residual energy from an accelerated test condition to the original reference test performed at the start of the procedure. Further, evidence that cells were physically damaged as a

consequence of the accelerated measurements would undermine the ethos of the test approach and reduce the feasibility of its introduction within a broader circular economy strategy for managing EOL vehicle battery systems.

6 Results

6.1 Experimental Error Analysis

To improve the efficacy of the results obtained, six cells of each type (twelve in total) were employed within the test programme. Based on a study of the relative accuracy of the experimental facilities employed within the laboratory and the manufacturing tolerances of the cell types used (e.g. variations in measured OCV and impedance) a sample size of 6 for each cell type was selected. This sample size provides a mean measurement error of 1.13% and 0.34% for the pouch and 18650 cells respectively. The results presented in the following subsections highlight the region of measurement uncertainty the arises from this potential measurement error. The numerical results presented in Tables 4 and 5 show the arithmetic mean value of energy capacity. For each test condition, the standard deviation is provided to highlight the spread of values across the samples of 6 cells.

6.2 Accelerated Measurement of Residual Stored Energy

Table 4 and 5 present the measured capacity values (averaged over the six cells) for the pouch cells and the 18650 cells for the different test conditions. Both Tables highlight the variations in the measured cell capacity as a function of the C-rate, the wait time allowed between successive charge and discharge events and the temperature of the cell when the capacity was measured. For each test case, the energy capacity recorded under the corresponding reference conditions is also highlighted. Figures 6 and 7 present the deviation of the measured cell capacity values with the

energy capacity measured under referenced test conditions. The figures highlight the region of uncertainty associated with the measurement error for each cell type. It can be seen that there is a greater variability in the residual energy measured as a function of cell temperature, than for the C-rate and the associated wait times. For example, for the test condition (C-Rate = 1C and wait time = 60 minutes) the average value of residual energy measured within the pouch cell varies from 40.82 Ah through to 31.81 Ah as cell temperature is changed from 40^0C to 0^0. Conversely, for a defined cell temperature (e.g. 25^0C), Figure 6 show that variations in the measured energy capacity are within the range of 0.48% under-estimation - 0.66% over-estimation for the different C-rates and wait times respectively.

6.3 Cell Degradation

Figures 8 and 9 presents the measured residual capacity for each cell (measured after electrically loading the cell with a given C-rate) relative to the initial reference value for the pouch and 18650 cells respectively. In addition, the region of uncertainty within the results from the measurement error is highlighted. For the pouch cell, the results shown in Figure 8 indicate that for ambient temperature conditions of 25^0C and 40^0C there is negligible capacity fade (e.g. at 40^0C the difference lies within the region of measurement error and for a temperature equal to 25^0C the maximum difference is only 1.41%). However, under cold temperature conditions, in particular when the cell is cycled at a high electrical load, significant performance degradation can be observed. As a direct consequence of the cell being cycled at its maximum C-rate at zero degrees, the cells experiences an average 8.6% reduction in energy capacity. This result is consistent with a number of other publications that address the topic of Li-ion cell degradation and discuss the possible causality between low temperature, high current and the occurrence of lithium plating [53,54] and high temperature and high current and the growth of the solid electrolyte interphase

layer growth [54]. From Figure 9, similar conclusions for the 18650 cell type may be made. At ambient temperatures of 25^0C and 40^0C, the measured reduction in cell capacity, experienced after cycling the cell at the highest C-rate was found to be between circa: 0.94-2.06%. Conversely, considerable capacity increase can be observed when cycling the cell at low temperatures, where a capacity increase of between 0.3 - 1% was recorded due to the cell warming effect reported in [17].

6.4 Timing Saving from the Reference Test Condition

Figure 10 presents the time saving possible when accelerating the energy capacity measurements. Data is presented as a percentage relative to the reference test condition for both pouch and 18650 cells for an ambient temperature of T=25^0C. The values shown represent those actually measured during test programme and therefore include the variable time element associated with the CV phase of the charge-cycle. The reference test, defined in [44] requires the use of wait times of 180 minutes for a change in cell SOC through a charge or discharge event. The reference test includes a wait step, charge step, another wait step and discharge step to measure cell capacity. The total time therefore required to complete a reference energy measurement test is circa: 614 minutes. It is noteworthy, that in order to better isolate the causality between measurement accuracy and the voltage relaxation time, defined in [44], for the cell to soak at the desired test temperature was unchanged.

7 Discussion

7.1 Optimizing the Relationship between Capacity Test Time and Accuracy

Table 6 presents the different test cases, defined in Figures 11 and 12 with each test allocated a unique number between one and nine. Tests are ranked in ascending order in terms of the time required for their completion. It is possible to combine the relative measures of test time and accuracy with the cost function:

$$J = \alpha.\widetilde{A_c} + \beta.\widetilde{t_c} \quad (1)$$

Where $\widetilde{A_c}$ defines the normalized accuracy of the accelerated test condition:

$$A_C = \frac{|C_R - C_A|}{Max(C)} \quad (2)$$

in which C_R and C_A denote the measured capacity from the reference test case and the accelerated test condition respectively. The term $\widetilde{t_c}$ defines the duration of the corresponding test case. The coefficients α and β are weighting factors that can be applied by organizations to express the relative importance of experimental accuracy verses test duration. For example, Figure 11 presents the cost function J for each test case, defined in Table 6 for the pouch cell, when both α and β have an equal value of 0.5. For these requirements, the optimal test parameters are those defined by test case 3 in which the cells are electrically cycled at 3C with wait-times of 30 minutes between successive charge-discharge events. The test duration is 50 minutes with an estimated accuracy 0.18% under-estimation when compared to the reference test condition (defined by Standard IEC 62660-1) that would require a test duration of 240 minutes (when the discharge time and wait time before the discharge is considered only). For another scenario, the relative weighting of α and β is changed to 0.2 and 0.8 respectively to emphasis the relative importance of process efficiency as opposed to absolute test accuracy.

Figure 12 highlights that the optimal parameters for the pouch cell have changed to those defined by test condition 1 from Table 5, namely a C-rate of 3C with a weight times of 0 minutes after each SOC adjustment. The test duration is now 20 minutes with an estimated accuracy of 0.7% over-estimation when compared to the reference test condition (defined by Standard EC 62660-1) corresponding to a reduction in testing time of circa: 220%. These scenarios highlight the flexibility of the approach in which different organizations could prioritize the relative importance of test accuracy verses experimental time when sorting/grading Li-ion cells for different EOL applications. However, irrespective of the final test parameters selected, the results presented in Tables 4 and 5 highlight that a significant reduction in test time (and thus cost and energy requirements) are achievable when compared to the experimental methods defined within current international battery test standards for Li-ion characterization.

7.2 Cell Damage

It is noteworthy that significant damage occurred to the pouch (power) cells during low temperature cycling. When the cell temperature was raised back to 25^0C to complete the monitoring characterization (to assess cell degradation) significant swelling was observed within three of the six cells. Figure 13 presents an example pouch cell showing clear signs of mechanical deformation. Due to safety concerns, the reference test was not performed on these cells. Throughout the experimental programme, no cell failures were observed with the 18650 energy cells. These results highlight the potential hazards associated with attempting to compress the energy measurement process too far. A number of publications discuss the relative degradation of Li-ion cells due to storage or calendar ageing [31,32]. Studies discuss that reduced calendar ageing is often observed with cells stored at lower temperatures [55,56]. For example, in [56] a high power 12Ah Kokam cell capacity reduced by 50% over 500 days when stored at 60^0C compared to

the 10% reduction in capacity when the cell is stored at 10^0C over the same period. These results imply that within a circular economy strategy, in which Li-ion cells are stored at lower temperatures to reduce ageing, the temperature of the cells should be raised before accelerated energy measurements are made if permanent damage within the cell is to be avoided. This constraint implies that either greater time must be allocated within the cell sorting/grading strategy for cell temperature to rise naturally or the OEM must incur the capital cost and greater running costs (including the associated CO_2 emissions) of warming the cells prior to commencing the accelerated test programme.

7.3 Further work

The results highlight that it is feasible to reduce the test duration required to assess the energy capacity (and thus SOH) for a Li-ion cell while still retaining levels of measurement accuracy that would support decision-making at battery EOL. Broadening the experimental programme to include cells from a wider cross-section of manufacturers and chemistries will further highlight the transferability of these results to other cell technologies. Based on these results the authors are currently investigating two primary areas of further work. The first, is to assess the scalability of this framework. It is probable that vehicle OEMs and specialist suppliers will seek to grade EV batteries at the module or pack level, rather than at the cell level. Research is therefore required to ascertain if the same levels of test accuracy are achievable with comparable levels of test time compression when characterizing complete battery modules or pack assemblies. Secondly, another measure often cited to quantify battery SOH is a rise in cell impedance. The test standards defined in Table 2 also include procedures for measuring cell impedance for different ambient temperatures and SOC. Research is currently ongoing to assess whether these procedures, most

notably the time allocated for the cell to stabilize after each SOC correction can be reduced, thereby improving the efficiency of the impedance characterization process.

8 Conclusions

Underpinning a number of studies that critically evaluate different circular economy strategies for the vehicle battery system are implicit assumptions about the retained capacity within the battery and thus it's SOH. Legislative and best-practice standards exist that address the performance evaluation requirements for the both EV and HEV battery systems. However, their test time requirements vary considerably depending on the exact nature of the test strategy; including the number of test points defined for battery SOC and temperature and the time defined to allow the battery voltage to stabilize after each change in SOC and after any charge or discharge event. The authors assert that these test durations would be prohibitive for a number of vehicle manufacturers and specialist energy storage suppliers wishing to sort or grade used vehicle battery systems to ascertain the most appropriate circular economy strategy for the battery. Experimental results are presented for two cell types and form-factor, that highlight that it is possible to significantly reduce the duration of the characterisation test (circa: 70-90% reduction) while still retaining levels of measurement accuracy in the order of 1% for cell temperatures of 25^0C. Even at elevated temperatures of 40^0C, the peak measurement error for the pouch cell was found to be circa: 3%. Only at low temperatures was measurement accuracy and cell degradation deemed to be so high as to prohibit its inclusion within a viable EOL battery strategy. A simple cost-function was formulated to highlight the flexibility of the approach in which different organizations could prioritize the relative importance of test accuracy verses experimental time when sorting/grading Li-ion cells for different EOL applications.

9 Figure Captions

Figure 1: Capacity test durations defined within international standards [44,57–59]

Figure 2: (a) Schematic representation of the experimental set-up; (b) Photograph of the experimental set-up (c) Photograph of the cell mounting fixture

Figure 3: Cell temperature measurement locations for both the 18650 and pouch cells

Figure 4: Overview of the experimental study

Figure 5: (a) Experimental test matrix completed; (b) Subset of the current profile applied to the cells under test

Figure 6: Average difference in measured capacity between the reference value and that measured for higher C-rates and reduced relation times for the pouch (power) cell

Figure 7: Average difference in measured capacity between the reference value and that measured for higher C-rates and reduced relation times for the 18650 (energy) cell

Figure 8: Measured cell degradation, averaged over each cell, for the pouch (power) cell

Figure 9: Measured cell degradation, averaged over each cell, for the 18650 (energy) cell

Figure 10: Time saving possible from accelerated energy capacity measurements (a) Pouch cell; (b) 18650 cell

Figure 11: Optimal selection of the accelerated energy capacity test ($\alpha = 0.5, \beta = 0.5$)

Figure 12: Optimal selection of the accelerated energy capacity test ($\alpha = 0.2, \beta = 0.8$)

Figure 13: Mechanical deformation of a pouch cell after low temperature, high current, testing

10 Tables

Nissan Leaf Battery System Overview									
Module Stack 1		**Module Stack 2**		**Module Stack 3**		**Mechanical Subsystems**		**Mechanical Subsystems**	
Item	**Quantity**	**Item**	**Quantity**	**Item**	**Quantity**	**Item**	**Quantity**	**Item**	**Quantity**
Modules	12	Modules	12	Modules	24	Compression Test Plug	1	BMS	1
Enclosures	24	Enclosures	24	Enclosures	48	Enclosures	2	BMS Mounting Bracket	1
Inner Cell Bundles	12	Inner Cell Bundles	12	Inner Cell Bundles	24	Cross-member Support	3	BMS Casing	2
Insulation sheets	24	Insulation sheets	24	Insulation sheets	48	Wiring Harness Brackets	4	Enclosures (Top/Bottom)	2
Metal Inserts	48	Metal Inserts	48	Metal Inserts	96	Seal	1	Bus Bar	4
Spaces	24	Spaces	24	Spaces	48			Current Sensor	1
Terminal Protection	12	Terminal Protection	12	Terminal Protection	24			Wiring Harness	1
Front Brackets	12	Front Brackets	12	Front Brackets	32			Relay Bracket	1
Rear Brackets	4	Rear Brackets	4	Rear Brackets	16			High Voltage Bus Bar	4
Bus Bar Assembly	1	Bus Bar Assembly	1	Bus Bar Assembly	1			Wiring Support	2
Base Plate	1	Base Plate	1	Base Plate	1			Plug	1
Front and Rear Plate Assembly	2	Front and Rear Plate Assembly	2	Brackets	4			Fuse	1
				Sub-pack Restraining Bolts	4			Relays	3
								Temperature Sensors	3
								Spacer	1
								Resistor	1

Table 1: Overview of the Nissan Leaf battery system

Title	Description
US Advanced Battery Consortium (USABC) Electric Vehicle Battery Test Procedures Manual: 1996 (Updated in June 2015 Revision 3)	This manual summarizes the procedural information needed to perform the battery testing specified by the USABC. This manual provides the structure and standards to be used by all testing organizations, including the USABC developers, national laboratories, or other relevant test facilities. The specific procedures defined in this manual support the performance and life characterization of advanced battery devices under development for EV applications.
US Department of Energy Standard DOE/ID-11069	USABC FreedomCAR battery test manual for power-assisted hybrid electric vehicles. This standard defines a series of tests to characterize aspects of the performance or cycle life behavior of batteries for hybrid electric vehicle applications.
Idaho National Laboratory (INL) Battery Test Manual for Plug-in Hybrid Electric Vehicles: 2010	This battery test procedure manual was prepared for the United States Department of Energy (DOE), Office of Energy Efficiency and Renewable Energy (EERE), Vehicle Technologies Program. It is based on technical targets established for energy storage development projects aimed at meeting system level DOE goals for Plug-in Hybrid Electric Vehicles (PHEV). The specific procedures defined in this manual support the performance and life characterization of advanced battery devices under development for PHEV's.
SAE J2288:2008	This standard is for lifecycle testing of electric vehicle battery modules. This SAE recommended practice defines a standardised test method to determine the expected service life, in cycles, of electric vehicle battery modules.
ISO 12405:2014	ISO 12405:2014 consists of the following parts, under the general title Electrically propelled road vehicles — Test specification for lithium-ion traction battery packs and systems: • Part 1: High-power applications • Part 2: High-energy applications • Part 3: Safety performance requirements. This part of ISO 12405 provides specific test procedures and related requirements to ensure an appropriate and acceptable level of safety of lithium-ion battery systems specifically developed for propulsion of road vehicles.
IEC EN 62660:2010	IEC EN 62660 has 2 parts and a third part in draft form. The standard is as follows: IEC EN 62660-1 – Secondary batteries for the propulsion of electric road vehicles – Performance testing for lithium-ion cells. IEC EN 62660-2 – Secondary batteries for the propulsion of electric road vehicles – Reliability and abuse testing for lithium-ion cells. Draft: IEC 62660-3. Secondary lithium-ion cells for the propulsion of electric road vehicles - Part 3: Safety requirements of cells and modules. The UK equivalent Standard is: BS EN 62660:2011 and also consist of two parts and a third draft section. The standard is as follows: BS EN 62660-1:2011 - Secondary lithium-ion cells for the propulsion of electric road vehicles. Performance testing. BS EN 62660-2:2011 - Secondary lithium-ion cells for the propulsion of electric road vehicles. Reliability and abuse testing. Draft: BS EN 62660-3. Secondary lithium-ion cells for the propulsion of electric road vehicles. Part 3. Safety requirements of cells and modules.
IEC EN 62281:2012	This standard specifies test methods and requirements for primary and secondary (rechargeable) lithium cells and batteries to ensure their safety during transport other than for recycling or disposal. The UK equivalent standard is: BS EN 62281:2013 and is about safety of primary and

	secondary lithium cells and batteries during transport.
QC/T 743-2006:2006	This Chinese standard are for Lithium-ion batteries for electric vehicles: This standard specifies the requirements, test methods, inspection rules, marking, packaging, transportation and storage of lithium-ion batteries for electric vehicles.
UN 38.3 – UN Manual of Tests and Criteria: 2009	The Manual of Tests and Criteria contains criteria, test methods and procedures to be used for classification of dangerous goods according to the provisions of Parts 2 and 3 of the United Nations Recommendations on the Transport of Dangerous Goods, Model Regulations, as well as for chemicals presenting physical hazards according to the Globally Harmonized System of Classification and Labeling of Chemicals (GHS).

Table 2: Overview of legislative and best practice test standards for vehicle battery systems

Parameter	Pouch (Power Cell)	18650 (Energy Cell)
Nominal energy Capacity	40 Ah	2.98 Ah
Maximum continuous charge rate	3C	C/3
Maximum continuous discharge rate	8C	3C
Maximum cell voltage	4.2 V	4.2 V
Minimum cell voltage	2.7 V	2.5 V

Table 3: Electrical performance data for both the Pouch and 18650 cell types

Temperature (^{0}C)	Wait Time (min)	C-Rate					
		1C		Max-C/2		Max-C	
		Mean Capacity	Standard Deviation	Mean Capacity	Standard Deviation	Mean Capacity	Standard Deviation
25	0	39.29	0.086	39.21	0.103	39.31	0.228
25	30	39.29	0.091	39.15	0.082	38.96	0.123
25	60	39.24	0.090	39.12	0.082	38.84	0.098
25	180	39.5	0.095	39.56	0.081	39.58	0.084
Temperature (^{0}C)	Wait Time (min)	C-Rate					
		1C		Max-C/2		Max-C	
		Mean Capacity	Standard Deviation	Mean Capacity	Standard Deviation	Mean Capacity	Standard Deviation
40	0	40.82	0.280	40.72	0.491	40.71	0.465
40	30	40.85	0.263	40.72	0.522	40.59	0.505
40	60	40.82	0.237	40.68	0.546	40.51	0.542
25	180	40.67	0.375	40.69	0.578	40.64	0.555
Temperature (^{0}C)	Wait Time (min)	C-Rate					
		1C		Max-C/2		Max-C	
		Mean Capacity	Standard Deviation	Mean Capacity	Standard Deviation	Mean Capacity	Standard Deviation
0	0	31.89	0.557	32.14	0.917	31.69	2.232
0	30	31.83	0.492	31.88	0.716	31.04	2.362
0	60	31.81	0.481	31.76	0.607	31.05	1.930
25	180	31.72	0.477	31.20	0.732	29.59	1.844

Table 4: Average capacity values measured during the accelerated testing on the power (pouch) cell.

Temperature (^{0}C)	Wait Time (min)	C-Rate					
		1C		Max-C/2		Max-C	
		Mean Capacity	Standard Deviation	Mean Capacity	Standard Deviation	Mean Capacity	Standard Deviation
25	0	2.74	0.02	2.73	0.02	2.77	0.02
25	30	2.74	0.02	2.74	0.02	2.78	0.02
25	60	2.75	0.02	2.74	0.02	2.78	0.02
25	180	2.74	0.02	2.71	0.02	2.69	0.02
Temperature (^{0}C)	Wait Time (min)	C-Rate					
		1C		Max-C/2		Max-C	
		Mean Capacity	Standard Deviation	Mean Capacity	Standard Deviation	Mean Capacity	Standard Deviation
40	0	2.83	0.02	2.82	0.02	2.81	0.02
40	30	2.84	0.02	2.83	0.01	2.81	0.02
40	60	2.84	0.02	2.83	0.02	2.81	0.02
25	180	2.83	0.02	2.81	0.02	2.80	0.02
Temperature (^{0}C)	Wait Time (min)	C-Rate					
		1C		Max-C/2		Max-C	
		Mean Capacity	Standard Deviation	Mean Capacity	Standard Deviation	Mean Capacity	Standard Deviation
0	0	2.20	0.03	2.26	0.03	2.44	0.01
0	30	2.21	0.03	2.25	0.03	2.45	0.01
0	60	2.22	0.03	2.25	0.02	2.44	0.01
25	180	2.22	0.03	2.22	0.03	2.23	0.02

Table 5: Average capacity values measured during the accelerated testing on the energy (18650) cell.

Test Number	Description	Duration (minutes) cell
1	0 minutes wait Max C	20
2	0 minutes wait Max C/2	40
3	30 minutes wait Max C	50
4	0 minutes wait 1C	60
5	30 minutes wait Max C/2	70
6	60 minutes wait Max C	80
7	30 minutes wait 1C	90
8	60 minutes wait Max C/2	100
9	60 minutes wait 1C	120

Table 6: Nine test cases ranked from in order of test duration

11 References

[1] The Boston Consulting Group. Focus Batteries for Electric Cars. Outlook 2010:1–18.

[2] Lu L, Han X, Li J, Hua J, Ouyang M. A review on the key issues for lithium-ion battery management in electric vehicles. J Power Sources 2013;226:272–88. doi:10.1016/j.jpowsour.2012.10.060.

[3] Waag W, Fleischer C, Sauer DU. Critical review of the methods for monitoring of lithium-ion batteries in electric and hybrid vehicles. J Power Sources 2014;258:321–39. doi:10.1016/j.jpowsour.2014.02.064.

[4] Xu J, Mi CC, Cao B, Cao J. A new method to estimate the state of charge of lithium-ion batteries based on the battery impedance model. J Power Sources 2013;233:277–84. doi:10.1016/j.jpowsour.2013.01.094.

[5] Hooper JM, Marco J. Experimental modal analysis of lithium-ion pouch cells. J Power Sources 2015;285:247–59. doi:10.1016/j.jpowsour.2015.03.098.

[6] Ellen Macarthur Foundation, McKinsey & Company. Towards the Circular Economy : Accelerating the scale-up across global supply chains. 2014.

[7] Thein S, Chang YS. Decision making model for lifecycle assessment of lithium-ion battery for electric vehicle – A case study for smart electric bus project in Korea. J Power Sources 2014;249:142–7. doi:10.1016/j.jpowsour.2013.10.078.

[8] Saxena S, Le Floch C, MacDonald J, Moura S. Quantifying EV battery end-of-life through analysis of travel needs with vehicle powertrain models. J Power Sources 2015;282:265–76. doi:10.1016/j.jpowsour.2015.01.072.

[9] Ziout A, Azab A, Atwan M. A holistic approach for decision on selection of end-of-life products recovery options. J Clean Prod 2014;65:497–516. doi:10.1016/j.jclepro.2013.10.001.

[10] Ahmadi L, Yip A, Fowler M, Young SB, Fraser RA. Environmental feasibility of re-use of electric vehicle batteries. Sustain Energy Technol Assessments 2014;6:64–74. doi:10.1016/j.seta.2014.01.006.

[11] Dubarry M, Truchot C, Liaw BY, Gering K, Sazhin S, Jamison D, et al. Evaluation of commercial lithium-ion cells based on composite positive electrode for plug-in hybrid electric vehicle applications. Part II. Degradation mechanism under 2C cycle aging. J Power Sources 2011;196:10336–43. doi:10.1016/j.jpowsour.2011.08.078.

[12] Foster M, Isely P, Standridge CR, Hasan MM. Feasibility assessment of remanufacturing, repurposing, and recycling of end of vehicle application lithium-ion batteries. J Ind Eng Manag 2014;7:698–715. doi:10.3926/jiem.939.

[13] Schneider EL, Kindlein W, Souza S, Malfatti CF. Assessment and reuse of secondary batteries cells. J Power Sources 2009;189:1264–9. doi:10.1016/j.jpowsour.2008.12.154.

[14] Neubauer J, Pesaran A. The ability of battery second use strategies to impact plug-in electric vehicle prices and serve utility energy storage applications. J Power Sources 2011;196:10351–8. doi:10.1016/j.jpowsour.2011.06.053.

[15] Ramoni MO, Zhang HC. End-of-life (EOL) issues and options for electric vehicle batteries. Clean Technol Environ Policy 2013;15:881–91. doi:10.1007/s10098-013-0588-4.

[16] Melissa Bowler, Bowler M. Battery Second Use : A Framework for Evaluating the Combination of Two Value Chains. All Diss 2014:1–32.

[17] Groenewald J, Marco J, Higgins N, Barai A. In-Service EV Battery Life Extension Through Feasible Remanufacturing. SAE World Congr. 2016, 2016, p. No. 2016-01-1290.

[18] Becker D. KPMG's Global Automotive Executive Survey 2015 2015.

[19] Santhanagopalan, Shriram and REW. Quantifying cell-to-cell variations in lithium ion batteries. Int J Electrochem 2012;2012:10. doi:http://dx.doi.org/10.1155/2012/395838.

[20] Hannan MA, Azidin FA, Mohamed A. Hybrid electric vehicles and their challenges: A review.

Renew Sustain Energy Rev 2014;29:135–50. doi:10.1016/j.rser.2013.08.097.

[21] BSI. BS8877-1:Design for manufacture, assembly, disassembly and end-of-life processing (MADE) - Part 1. Br Stand Inst 2006. http://shop.bsigroup.com/en/ProductDetail/?pid=000000000030218703.

[22] Fang HC, Ong SK, Nee AYC. Product Remanufacturability Assessment based on Design Information. Procedia CIRP 2014;15:195–200. doi:10.1016/j.procir.2014.06.050.

[23] Hendrickson TP, Kavvada O, Shah N, Sathre R, D Scown C. Life-cycle implications and supply chain logistics of electric vehicle battery recycling in California. Environ Res Lett 2015;10:14011. doi:10.1088/1748-9326/10/1/014011.

[24] Schau EM, Traverso M, Lehmannann A, Finkbeiner M. Life cycle costing in sustainability assessment-A case study of remanufactured alternators. Sustainability 2011;3:2268–88. doi:10.3390/su3112268.

[25] Zackrisson M, Avellán L, Orlenius J. Life cycle assessment of lithium-ion batteries for plug-in hybrid electric vehicles – Critical issues. J Clean Prod 2010;18:1519–29. doi:10.1016/j.jclepro.2010.06.004.

[26] Long E, Kokke S, Lundie D, Shaw N, Ijomah W, Kao C. Technical solutions to improve global sustainable management of waste electrical and electronic equipment (WEEE) in the EU and China. J Remanufacturing 2016;6:1–27. doi:10.1186/s13243-015-0023-6.

[27] Ijomah WL, McMahon CA, Hammond GP, Newman ST. Development of design for remanufacturing guidelines to support sustainable manufacturing. Robot Comput Integr Manuf 2007;23:712–9. doi:10.1016/j.rcim.2007.02.017.

[28] Marshall SE, Archibald TW. Substitution in a Hybrid Remanufacturing System. Procedia CIRP 2015;26:583–8. doi:10.1016/j.procir.2014.07.073.

[29] Bras B, Hammond R. Towards Design for Remanufacturing – Metrics for Assessing Remanufacturability 1996:5–22.

[30] Goodall P, Rosamond E, Harding J. A review of the state of the art in tools and techniques used to evaluate remanufacturing feasibility. J Clean Prod 2014;81:1–15. doi:10.1016/j.jclepro.2014.06.014.

[31] Schuster SF, Brand MJ, Campestrini C, Gleissenberger M, Jossen A. Correlation between capacity and impedance of lithium-ion cells during calendar and cycle life. J Power Sources 2016;305:191–9. doi:10.1016/j.jpowsour.2015.11.096.

[32] Broussely M, Herreyre S, Biensan P, Kasztejna P, Nechev K, Staniewicz R. Aging mechanism in Li ion cells and calendar life predictions. J Power Sources 2001;97–98:13–21. doi:10.1016/S0378-7753(01)00722-4.

[33] Ning G, Haran B, Popov BN. Capacity fade study of lithium-ion batteries cycled at high discharge rates. J Power Sources 2003;117:160–9. doi:10.1016/S0378-7753(03)00029-6.

[34] Lin X, Stefanopoulou AG, Li Y, Anderson RD. State of Charge Estimation of Cells in Series Connection by Using only the Total Voltage Measurement 2013.

[35] Pastor-Fernández C, Bruen T, Widanage WD, Gama-Valdez MA, Marco J. A Study of Cell-to-Cell Interactions and Degradation in Parallel Strings: Implications for the Battery Management System. J Power Sources 2016;329:574–85. doi:10.1016/j.jpowsour.2016.07.121.

[36] Guenther C, Schott B, Hennings W, Waldowski P, Danzer MA. Model-based investigation of electric vehicle battery aging by means of vehicle-to-grid scenario simulations. J Power Sources 2013;239:604–10. doi:10.1016/j.jpowsour.2013.02.041.

[37] Farmann A, Waag W, Marongiu A, Sauer DU. Critical review of on-board capacity estimation techniques for lithium-ion batteries in electric and hybrid electric vehicles. J Power Sources 2015;281:114–30. doi:10.1016/j.jpowsour.2015.01.129.

[38] Wong D, Shrestha B, Wetz DA, Heinzel JM. Impact of high rate discharge on the aging of lithium nickel cobalt aluminum oxide batteries. J Power Sources 2015;280:363–72.

doi:10.1016/j.jpowsour.2015.01.110.

[39] Jaguemont J, Boulon L, Dubé Y. A comprehensive review of lithium-ion batteries used in hybrid and electric vehicles at cold temperatures. Appl Energy 2016;164:99–114. doi:10.1016/j.apenergy.2015.11.034.

[40] Forgez C, Vinh Do D, Friedrich G, Morcrette M, Delacourt C. Thermal modeling of a cylindrical LiFePO4/graphite lithium-ion battery. J Power Sources 2010;195:2961–8. doi:10.1016/j.jpowsour.2009.10.105.

[41] Wang Q, Jiang B, Li B, Yan Y. A critical review of thermal management models and solutions of lithium-ion batteries for the development of pure electric vehicles. Renew Sustain Energy Rev 2016;64:106–28. doi:10.1016/j.rser.2016.05.033.

[42] Smith K, Wang C-Y. Solid-state diffusion limitations on pulse operation of a lithium ion cell for hybrid electric vehicles. J Power Sources 2006;161:628–39. doi:http://dx.doi.org/10.1016/j.jpowsour.2006.03.050.

[43] Lacey G, Jiang T, Putrus G, Kotter R. The effect of cycling on the state of health of the electric vehicle battery. Proc Univ Power Eng Conf 2013. doi:10.1109/UPEC.2013.6715031.

[44] IEC 62660-1:2010 specifies performance and life testing of secondary lithium-ion cells used for propulsion of electric vehicles including battery electric vehicles (BEV) and hybrid electric vehicles (HEV). 2010. http://www.iec.ch/.

[45] Chang MH, Huang HP, Chang SW. A new state of charge estimation method for LiFePO4 battery packs used in robots. Energies 2013;6:2007–30. doi:10.3390/en6042007.

[46] Zhong L, Zhang C, He Y, Chen Z. A method for the estimation of the battery pack state of charge based on in-pack cells uniformity analysis. Appl Energy 2014;113:558–64. doi:10.1016/j.apenergy.2013.08.008.

[47] Dubarry M, Devie A, Liaw BY. Cell-balancing currents in parallel strings of a battery system. J Power Sources 2016;321:36–46. doi:10.1016/j.jpowsour.2016.04.125.

[48] Bruen T, Marco J. Modelling and experimental evaluation of parallel connected lithium ion cells for an electric vehicle battery system. J Power Sources 2016;310:91–101. doi:http://dx.doi.org/10.1016/j.jpowsour.2016.01.001.

[49] Baccouche I, Mlayah A, Jemmali S, Manai B, Amara NE Ben. $implementation of a Coulomb counting algorithm for SOC estimation of Li-Ion battery for multimedia applications. 12th Int Multi-Conference Syst Signals Devices, SSD 2015 2015:1–6. doi:10.1109/SSD.2015.7348255.

[50] Plett GL. Extended Kalman filtering for battery management systems of LiPB-based HEV battery packs: Part 3. State and parameter estimation. J Power Sources 2004;134:277–92. doi:http://dx.doi.org/10.1016/j.jpowsour.2004.02.033.

[51] Yuan S, Wu H, Yin C. State of charge estimation using the extended Kalman filter for battery management systems based on the ARX battery model. Energies 2013;6:444–70. doi:10.3390/en6010444.

[52] Barré A, Deguilhem B, Grolleau S, Gérard M, Suard F, Riu D. A review on lithium-ion battery ageing mechanisms and estimations for automotive applications. J Power Sources 2013;241:680–9. doi:10.1016/j.jpowsour.2013.05.040.

[53] Zhang SS. The effect of the charging protocol on the cycle life of a Li-ion battery. J Power Sources 2006;161:1385–91. doi:10.1016/j.jpowsour.2006.06.040.

[54] Zhang Y, Wang C-Y. Cycle-Life Characterization of Automotive Lithium-Ion Batteries with LiNiO[sub 2] Cathode. J Electrochem Soc 2009;156:A527. doi:10.1149/1.3126385.

[55] Amine K, Chen CH, Liu J, Hammond M, Jansen A, Dees D, et al. Factors responsible for impedance rise in high power lithium ion batteries. J Power Sources 2001;97–98:684–7. doi:10.1016/S0378-7753(01)00701-7.

[56] Eddahech A, Briat O, Woirgard E, Vinassa JM. Remaining useful life prediction of lithium batteries in calendar ageing for automotive applications. Microelectron Reliab 2012;52:2438–42. doi:10.1016/j.microrel.2012.06.085.

[57] ISO Standards Publication Electrically propelled road vehicles — Test specification for lithium-ion traction battery packs and systems 2012. https://www.iso.org/obp/ui/#iso:std:51414:en.

[58] USABC n.d. http://www.uscar.org/guest/article_view.php?articles_id=86.

[59] QC/T n.d. http://www.chinesestandard.net/List-PDF/QC.aspx.

Figure 1
Click here to download high resolution image

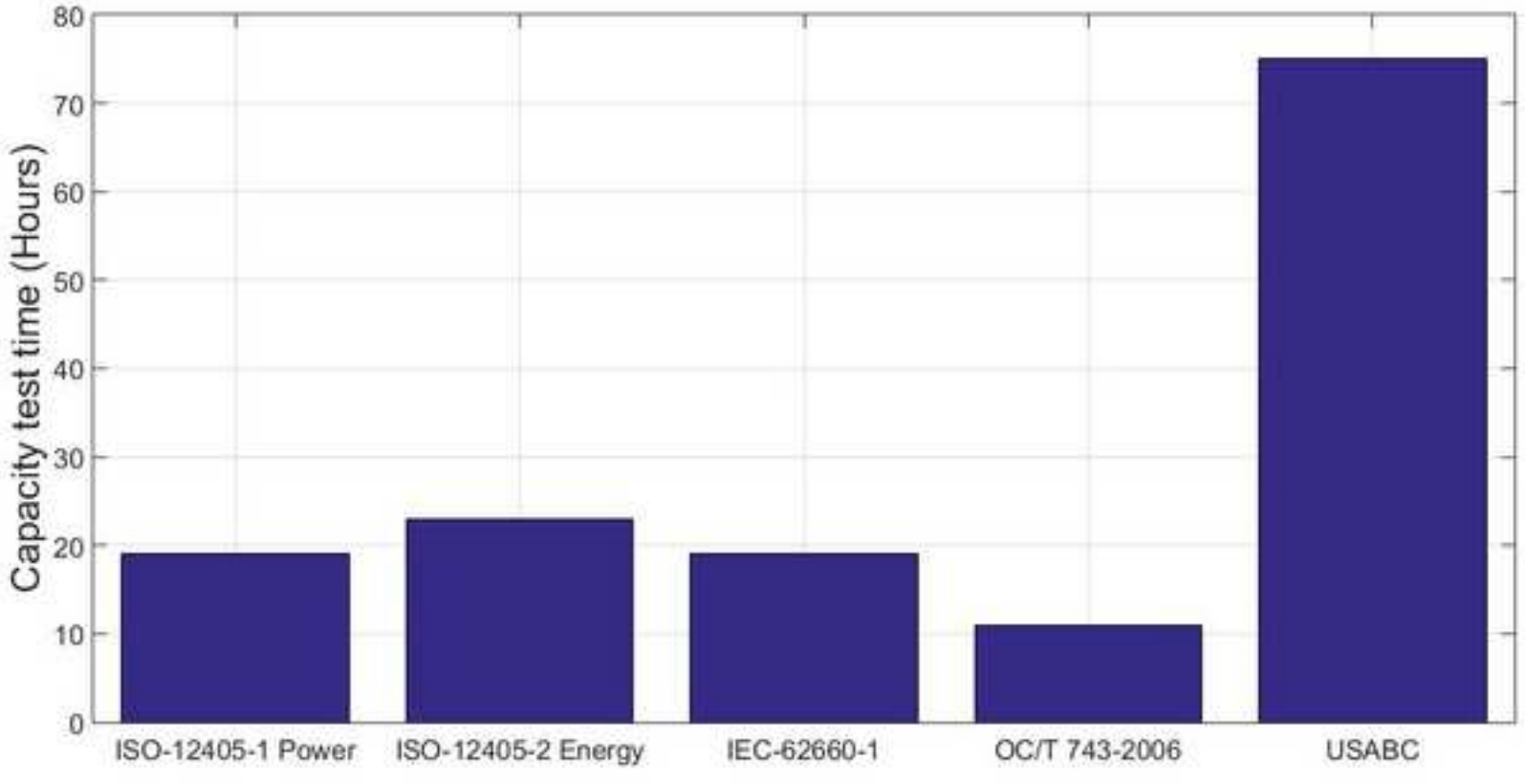

Figure 2 Revised

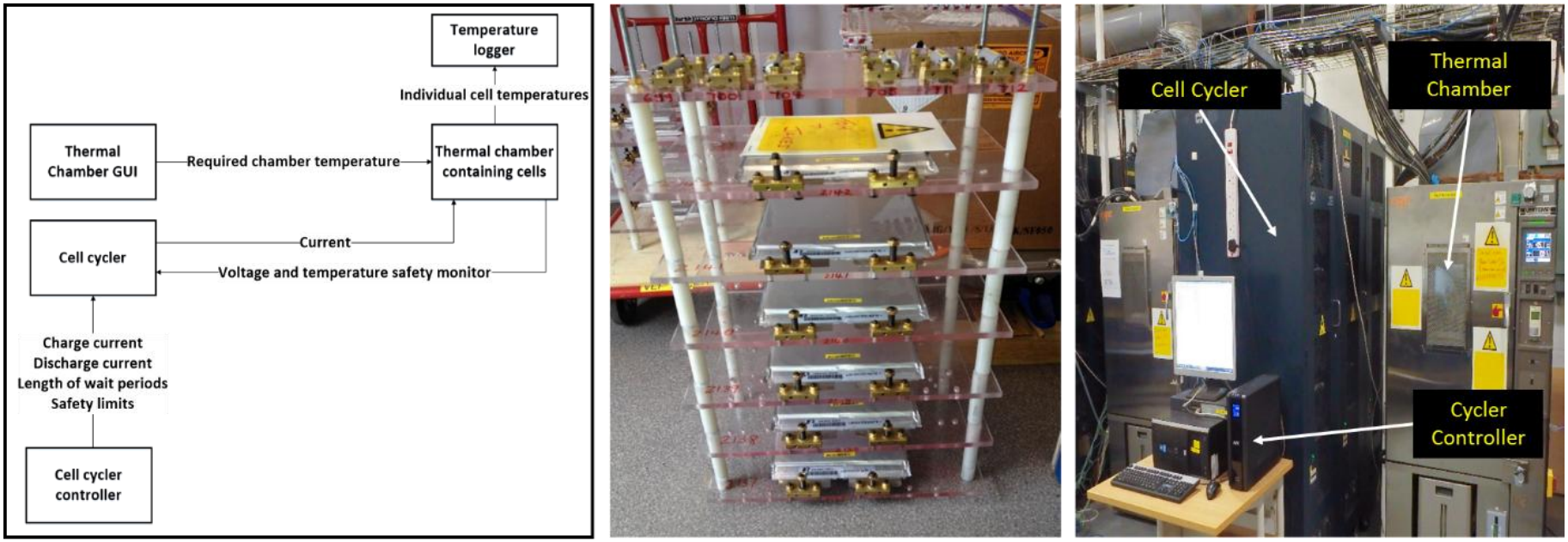

a b c

Figure 3

Click here to download high resolution image

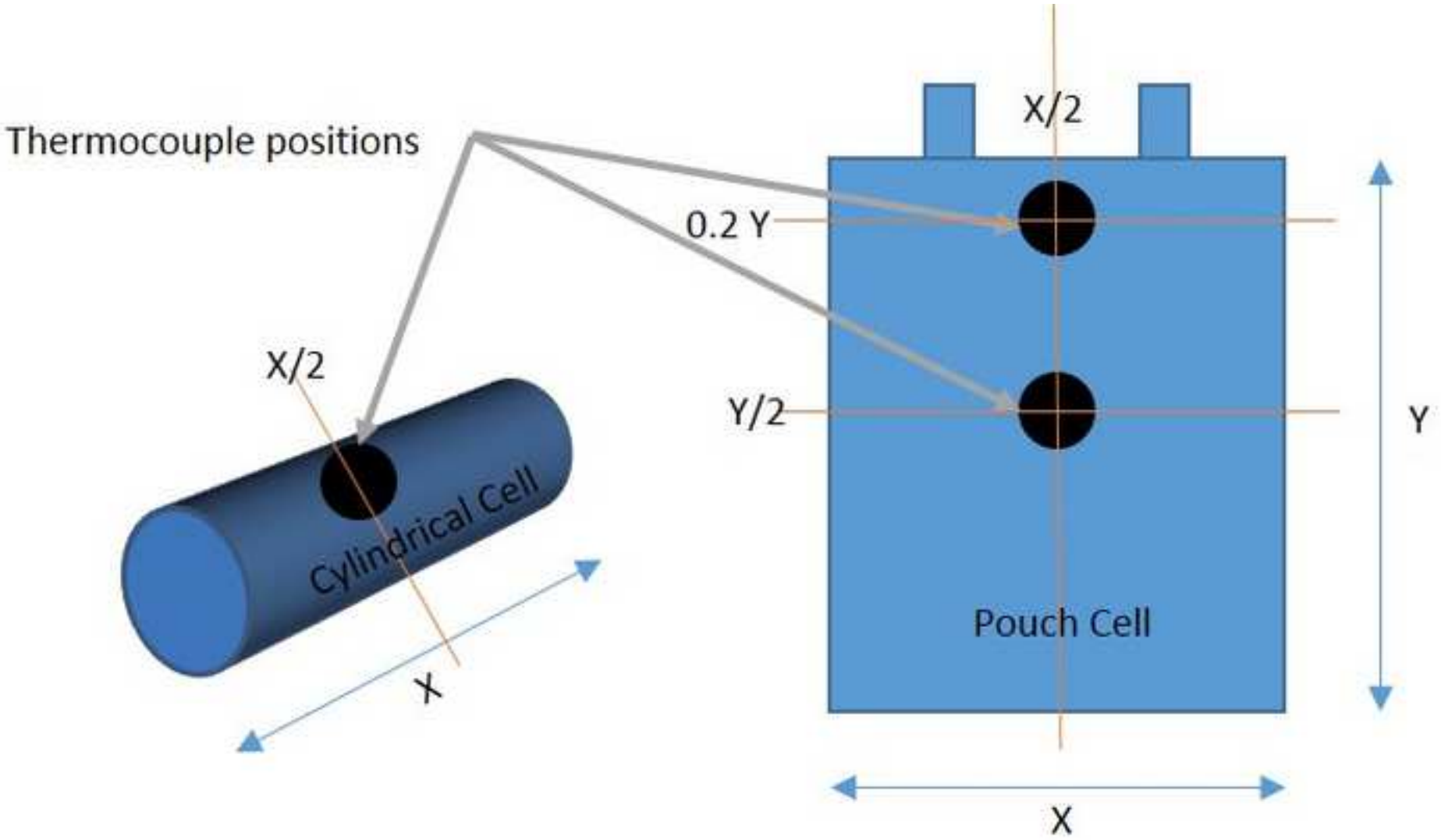

Figure 4

Click here to download high resolution image

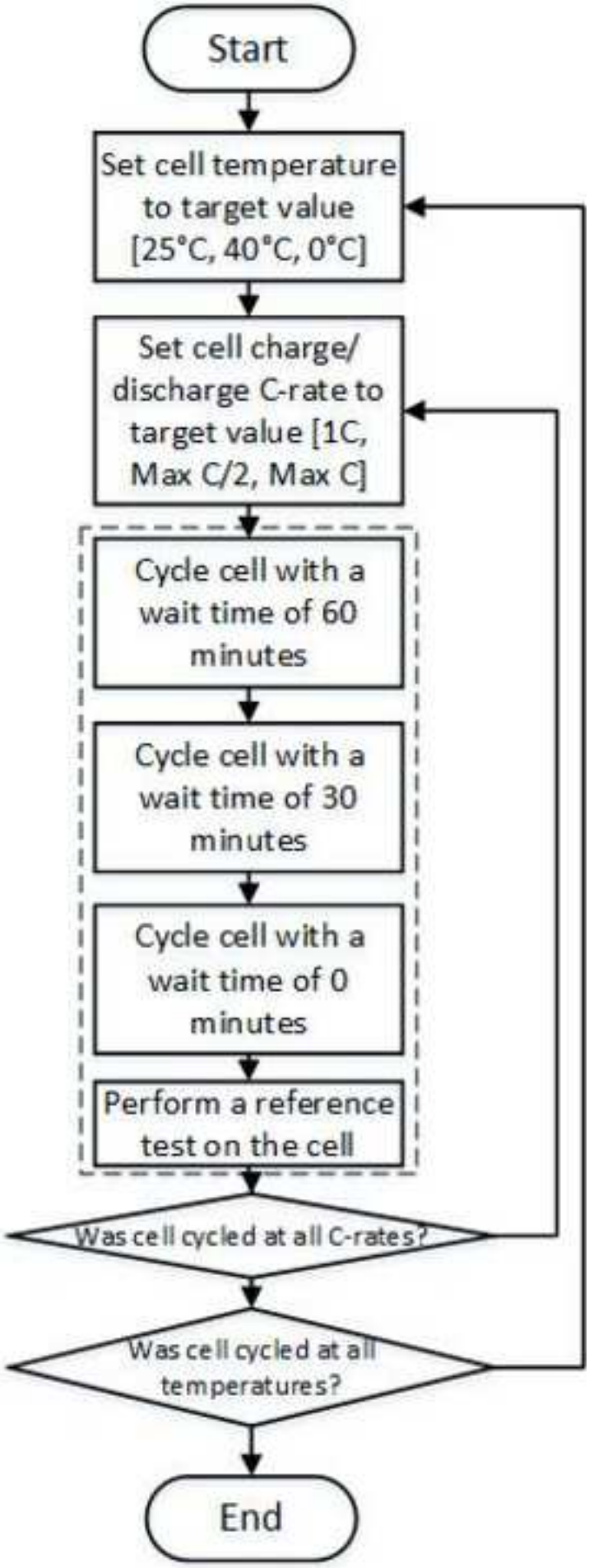

Figure 5

Click here to download high resolution image

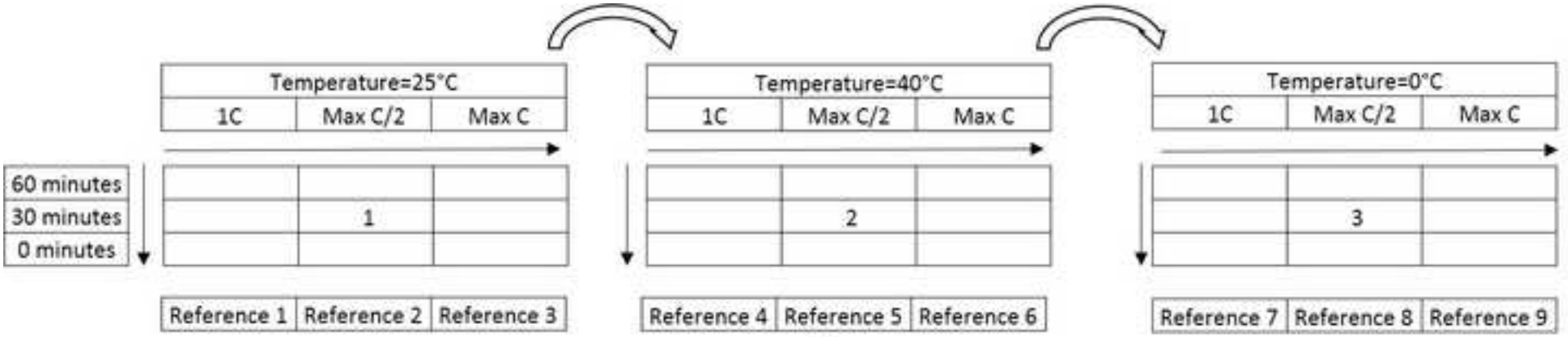

a

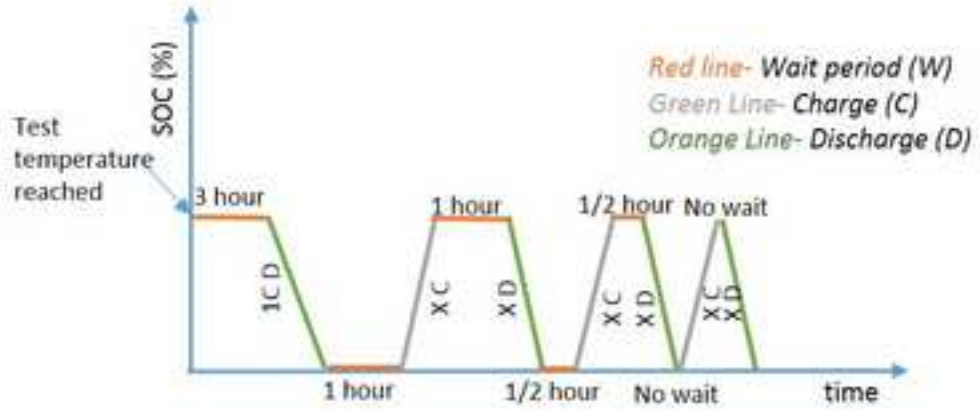

Repeat for 3 different C rates :1C, Max C/2, Max C

b

Figure 6

Click here to download high resolution image

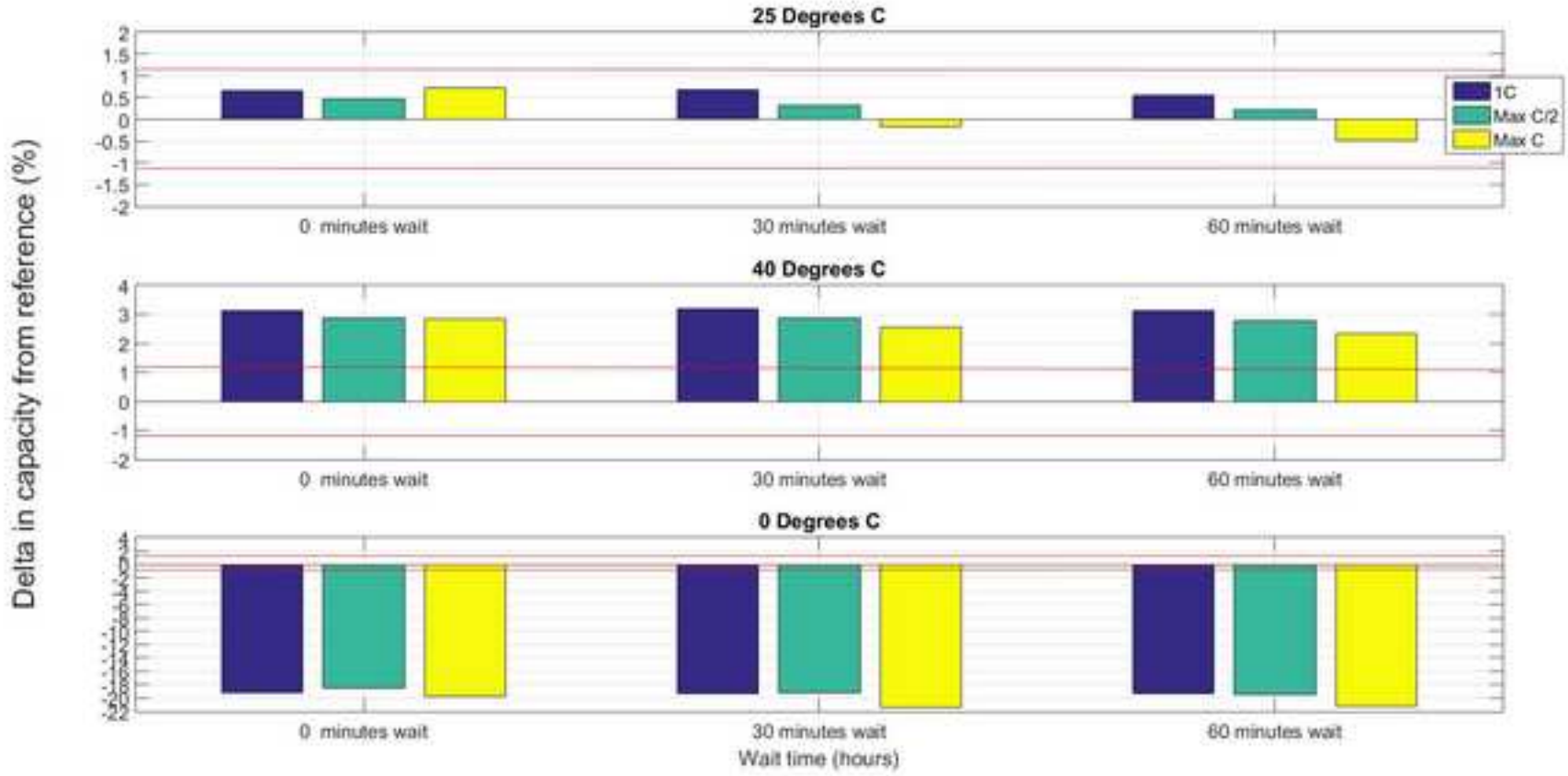

Figure 7

Click here to download high resolution image

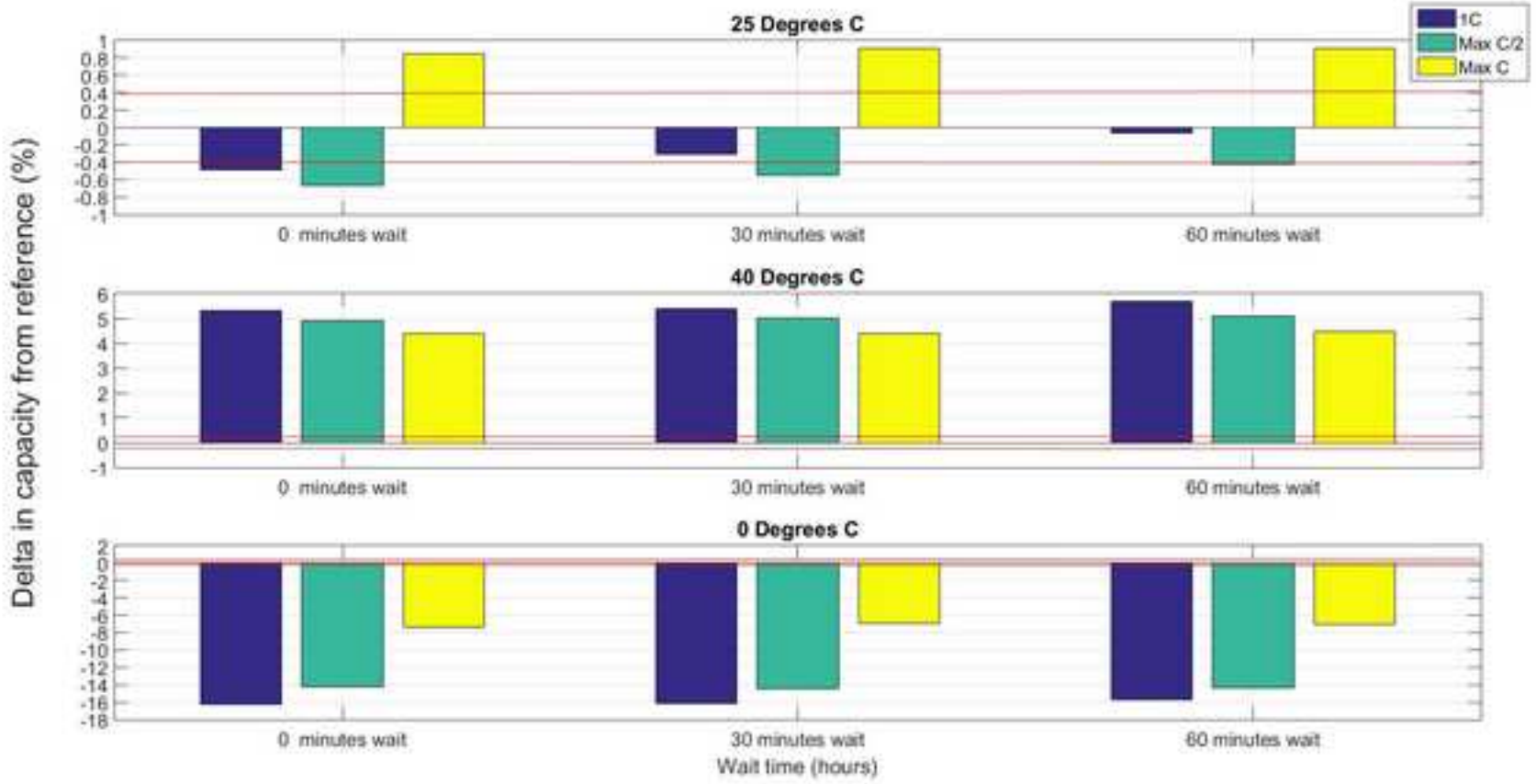

Figure 8

Click here to download high resolution image

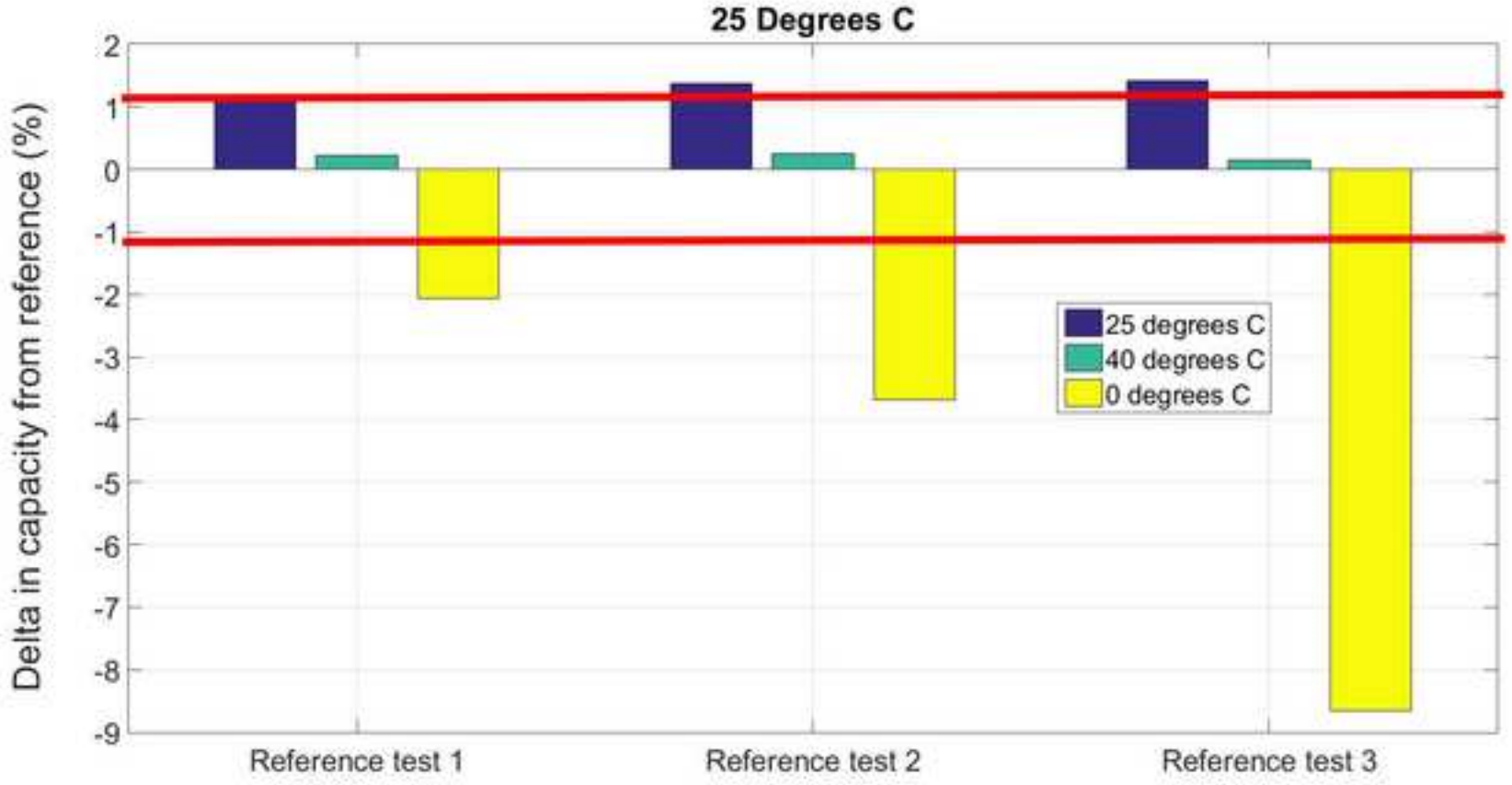

Figure 9

Click here to download high resolution image

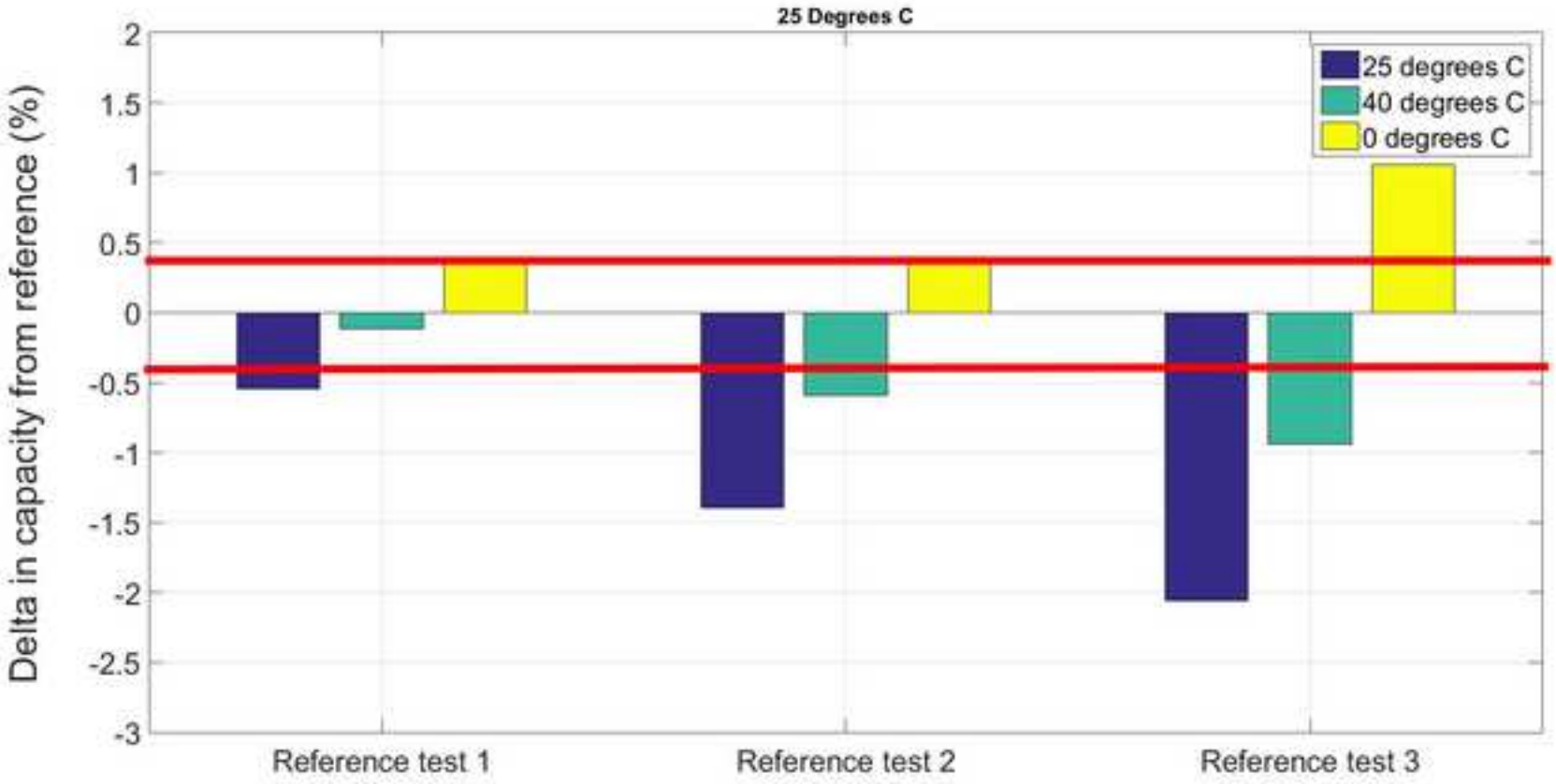

Figure 10

Click here to download high resolution image

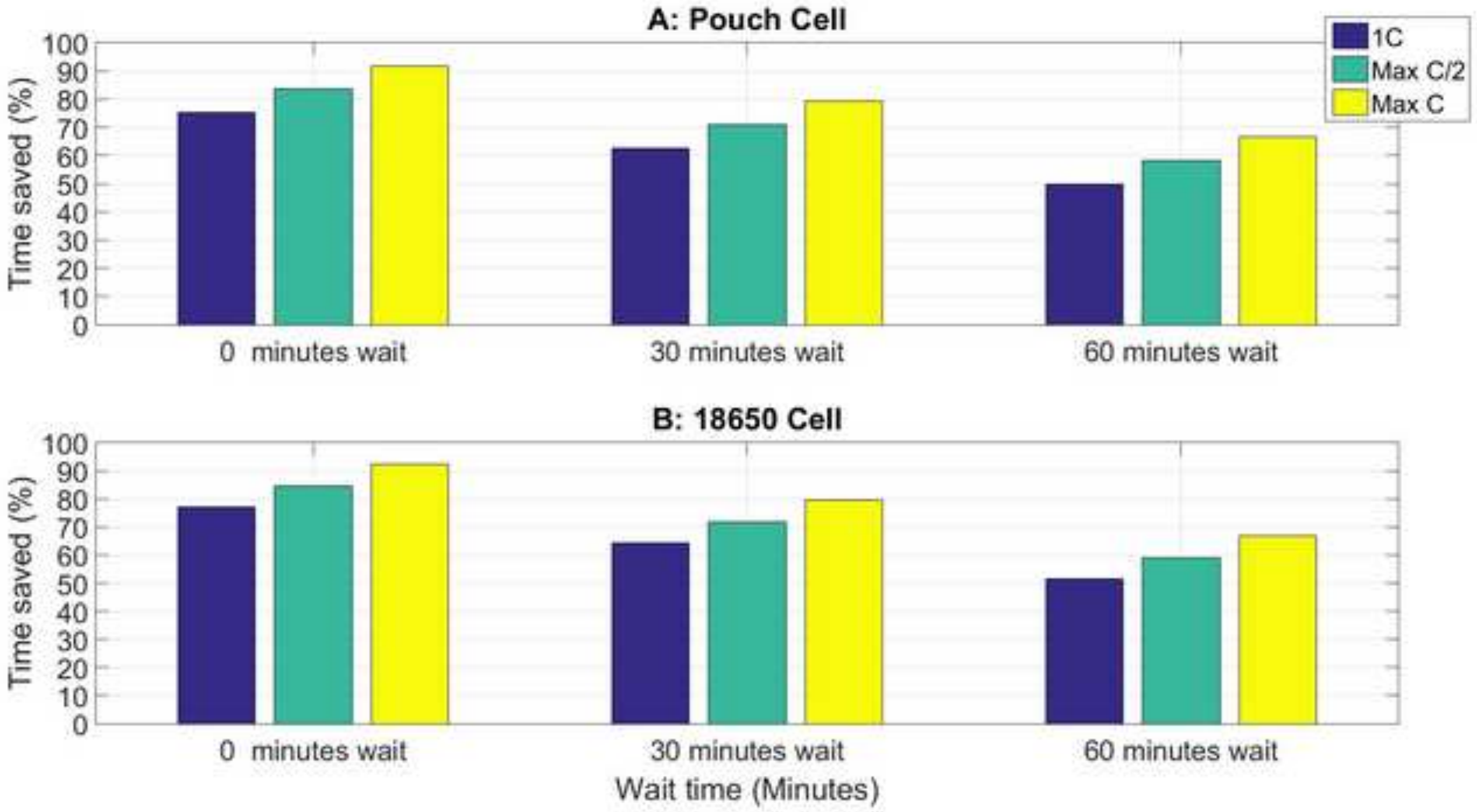

Figure 11

Click here to download high resolution image

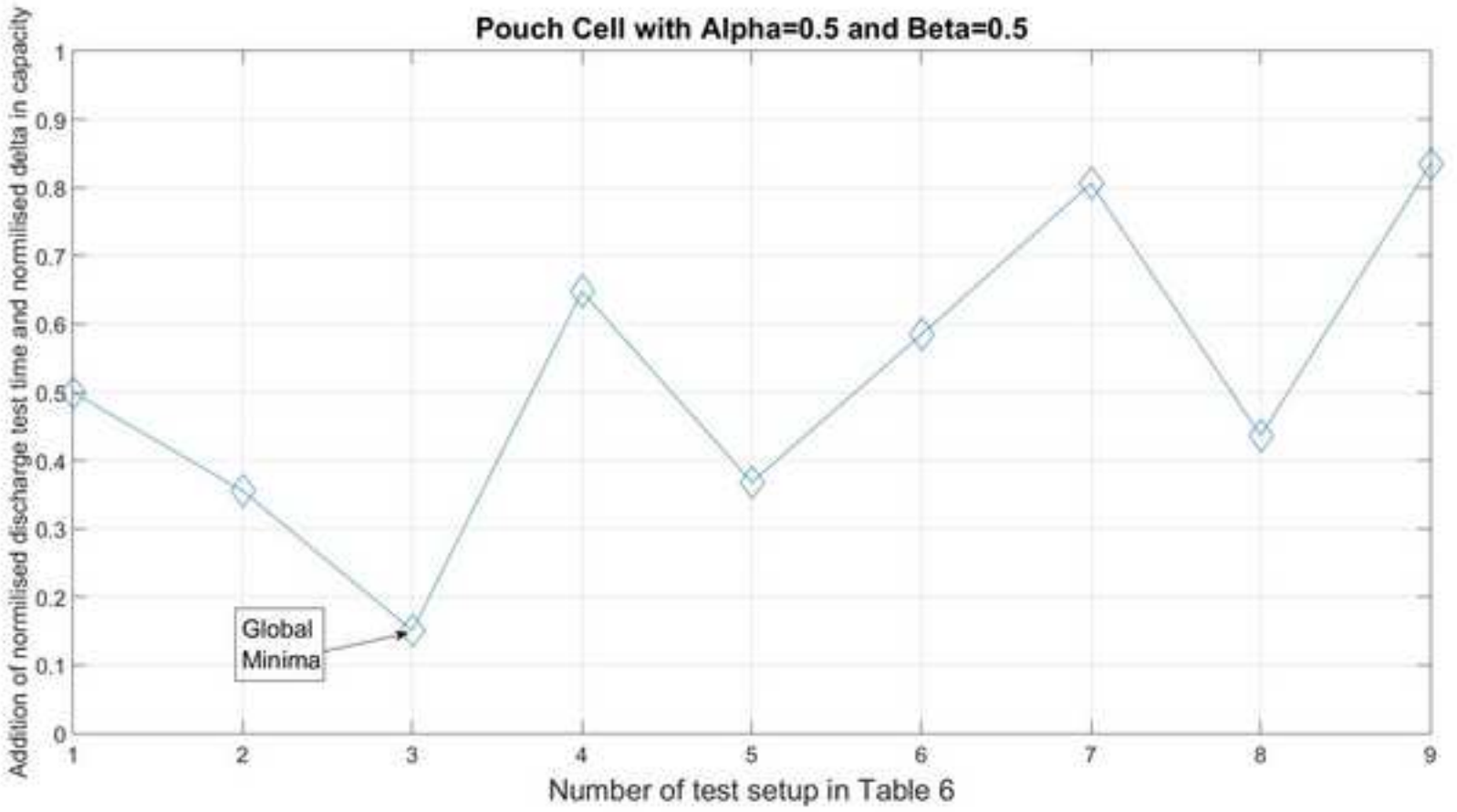

Figure 12

Click here to download high resolution image

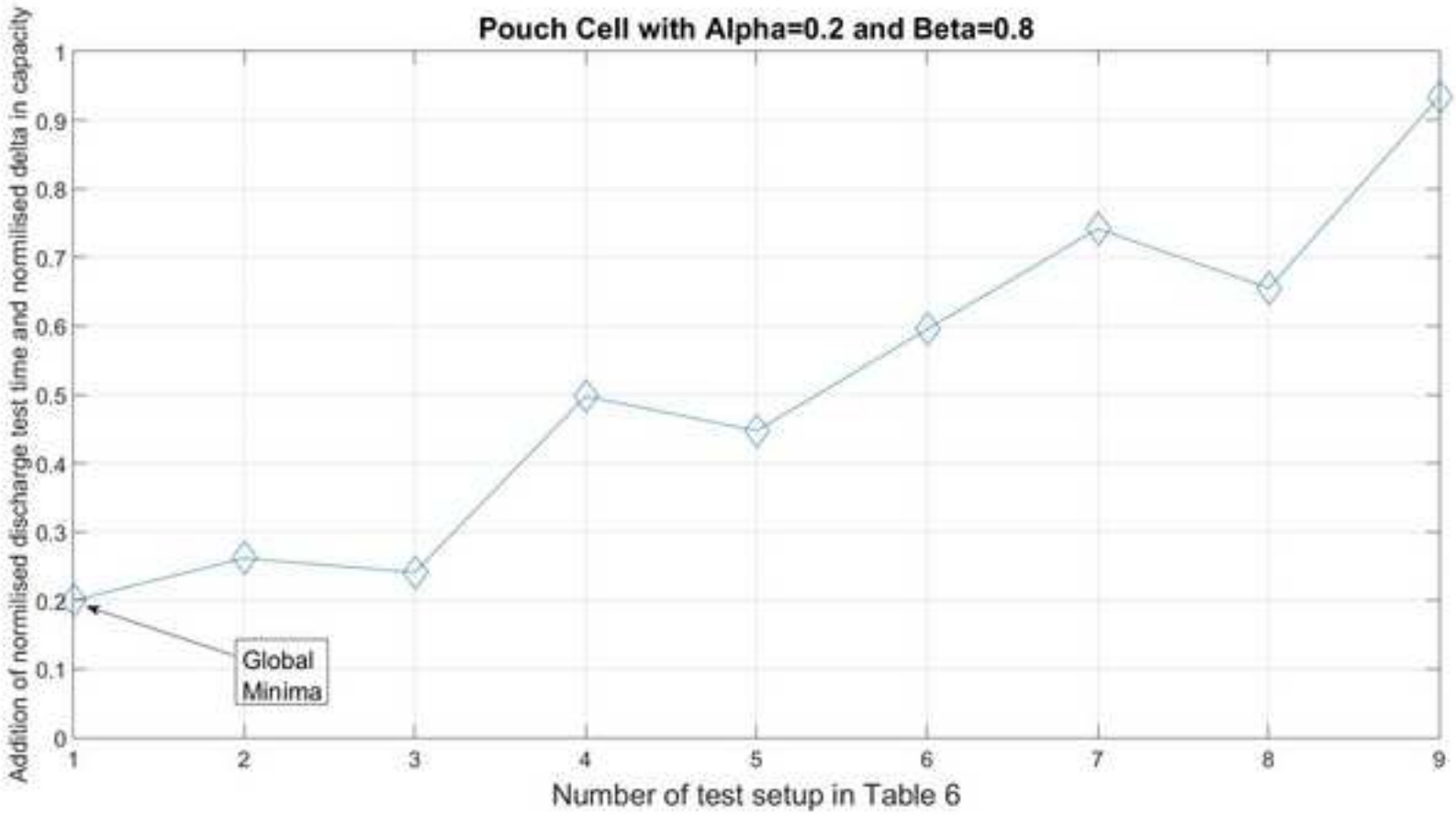

Figure 13

Click here to download high resolution image